Morphology Variation of Porous Polymer Gels by Polymerization in Lyotropic Surfactant Phases

Markus Antonietti,* Rachel A. Caruso, Christine G. Göltner, and Markus C. Weissenberger

Max Planck Institute of Colloids and Interfaces, Kantstrasse 55, D-14513 Teltow-Seehof, Germany

Received August 6, 1998; Revised Manuscript Received December 8, 1998

ABSTRACT: Polymerization of hydrophilic monomers, such as acrylamide, in the confinement of lyotropic liquid crystalline phases of nonionic surfactants produces gels with variable pore architecture in the hundreds of nanometers to micrometers size range. The porous gels are characterized by scanning electron microscopy after critical-point drying. The structure of the gels depends on the type of monomer, cross-linking density, and both monomer and surfactant concentration and can be varied systematically to result in different pore morphologies with different pore sizes. In such a way it is possible to build the polymer network structure on a mesoscopic length scale, optimizing different network properties which are otherwise coupled in an opposite fashion; e.g., polymer networks with very large pore size and high mechanical stability can be made.

I. Introduction

Hydrophilic polymer gels, such as polyacrylamide gels, belong to the most important class of functional polymers in modern biotechnology. A significant part of protein chemistry and genetic engineering relies on highly efficient separation processes, such as gel electrophoresis, which are performed within water-based polymer gels.[1] Despite this fact, the study of these gels is somewhat neglected by the scientific community, and surprisingly, optimization of the gel structure has thus far not been performed. These gels are still made by in-situ radical polymerization in water inside the separation devices.[1] This procedure has inherent limitations, since a number of network properties are inversely coupled. Separation of larger biological entities or DNA fragments requires, for instance, large pores, the synthesis of which classically relies on high water contents during polymerization and low cross-linking densities. This approach inevitably affords a mechanically very weak or soft gel, which in addition easily changes its degree of swelling. It is obvious that the use of such products, as well as the parameter range accessible by classical methods, is restricted.

From the viewpoint of supramolecular polymer science, it is a challenge to meet the demands of biotechnology by constructing polymer networks with a mesoscale architecture. Here, nanometer to micron size pores are separated by highly cross-linked polymer regions which provide sufficient mechanical stability. This strategy has been used for the generation of micron sized gel beads, where so-called macroporous separation particles are applied in chromatography and GPC.[2] Recently, Frechet et al. extended a similar technique to produce solid monolithic gels and column fillings of macroscopic size, using classical low molecular weight porogens such as hydrophobic alcohols.[3] The authors demonstrated the superb permeability and chromatographic separation of these gels.

To allow the direct use of such monolithic gels in classical separation setups without extensive adaptation of the process, a potential gel synthesis must focus on generating a complex polymer structure in a simple procedure from standard monomers. For this purpose, we propose a technique examined in the last few years by a number of work groups,[4−9] namely the polymerization in the continuous aqueous phase of a lyotropic liquid crystal. Here, monomer is dissolved in the water phase surrounding surfactant assemblies, ordered in a hexagonal, bicontinuous cubic, or lamellar fashion. Polymerization is performed to stabilize the ordered structure, and voids, formed by the surfactant assemblies and other nonpolymerizable components, displace the polymer growth.

The key problem in this approach is the preservation of the originally well-ordered phase structure, since the growing polymer chains influence the thermodynamic stability of the microemulsion or the lyotropic phase. Specific interactions as well as the entropy loss of a polymeric chain in a confined geometry usually result in the destruction of the nanometer-scale order; nevertheless, differently ordered products with interesting properties are obtained. Some of these problems have been recently reviewed in context with polymerization in microemulsions;[10,11] the loss of the mesomorphous order and the appearance of new structure patterns in the micrometer range were demonstrated for the polymerization in bicontinuous microemulsions containing hydrophobic as well as hydrophilic monomers by a variety of techniques.[12−16] The structures described in these papers are very close to those being advantageous for separation experiments, but a change toward a pure hydrophilic polymer backbone which does not (or only weakly) interact with biomolecules has to be considered. This is possible by switching from the ternary microemulsions to the less well examined binary lyotropic phases which do not contain hydrophobic monomers or oils.

In the present paper the polymerization of hydrophilic standard monomers, acrylamide, *N*-isopropylacrylamide, *N*,*N*-dimethylacrylamide, methacrylic acid glycidyl ester, and 2-hydroxyethyl methacrylate (HEMA), in the aqueous domains of lyotropic liquid crystalline phases of nonionic amphiphiles is presented. For the formation of surfactant assemblies, different nonionics have been chosen: Brij56 (main component: decaethylene glycol hexadecyl ether), Brij58 (main component:

10.1021/ma9812478 CCC: $18.00
Published on Web 02/12/1999

Table 1. Compositions of All the Gel Samples Discussed in This Examination

sample	monomer	surfactant	$m_{monomer}$ (g)	m_{H_2O} (g)	$m_{surfactant}$ (g)	$m_{X-linker}$ (g)
GAM-1	acrylamide	Brij56	3.0	6.0	0.6	0.2[a]
GAM-2	acrylamide	Brij56	3.0	6.0	1.2	0.2[a]
GAM-3	acrylamide	Brij56	3.0	6.0	1.8	0.2[a]
GAM-4	acrylamide	Brij56	3.0	6.0	2.4	0.2[a]
GAM-5	acrylamide	Brij56	3.0	6.0	3.0	0.2[a]
GAM-6	acrylamide	Brij56	3.0	6.0	3.6	0.2[a]
GNP-4	*N*-isopropylacrylamide	Brij56	3.0	6.0	1.0	0.2[a]
GNP-7	*N*-isopropylacrylamide	Brij56	3.0	6.0	1.5	0.2[a]
GNP-8	*N*-isopropylacrylamide	Brij56	3.0	6.0	2.0	0.2[a]
GNP-9	*N*-isopropylacrylamide	Brij56	3.0	6.0	2.5	0.2[a]
RNP-2	*N*-isopropylacrylamide	Brij56	3.0	6.0	3.0	0.4[a]
PNIP-No	*N*-isopropylacrylamide		3.0	6.0		0.4[a]
RAM-2	acrylamide	Brij56	3.0	6.0	3.0	0.4[a]
PAM-No	acrylamide		3.0	6.0		0.4[a]
RDA-2	*N*,*N*-dimethylacrylamide	Brij56	3.0	6.0	3.0	0.4[a]
PDM-No	*N*,*N*-dimethylacrylamide		3.0	6.0		0.4[a]
RHE-2	2-hydroxyethyl methacrylate	Brij56	3.0	6.0	3.0	0.4[b]
PHE-No	2-hydroxyethyl methacrylate		3.0	6.0		0.4[b]
BG-1	acrylic acid:methacrylic acid glycidyl ester 1:1	Brij58	2.0	8.0	1.0	0.2[b]
BG-2	acrylic acid:methacrylic acid glycidyl ester 1:1	Brij58	2.0	8.0	1.0	0.4[b]
BG-3	acrylic acid:methacrylic acid glycidyl ester 1:1	Brij58	2.0	8.0	1.0	0.6[b]
BG-4	acrylic acid:methacrylic acid glycidyl ester 1:1	Brij58	3.0	8.0	1.0	0.3[b]
BG-5	acrylic acid:methacrylic acid glycidyl ester 1:1	Brij58	3.0	8.0	1.0	0.6[b]
BG-6	acrylic acid:methacrylic acid glycidyl ester 1:1	Brij58	3.0	8.0	1.0	0.9[b]
BG-7	acrylic acid:methacrylic acid glycidyl ester 1:1	Brij58	4.0	8.0	1.0	0.4[b]
BG-8	acrylic acid:methacrylic acid glycidyl ester 1:1	Brij58	4.0	8.0	1.0	0.8[b]
BG-9	acrylic acid:methacrylic acid glycidyl ester 1:1	Brij58	4.0	8.0	1.0	1.2[b]
t1	acrylic acid:methacrylic acid glycidyl ester 1:1	Tween60	1.0	8.0	4.0	0.2[b]
t2	2-hydroxyethyl methacrylate	Tween60	2.0	8.0	4.0	0.2[b]
t3	*N*,*N*-dimethylacrylamide	Tween60	2.0	8.0	4.0	0.2[b]

[a] Bis(acrylamide). [b] Ethylene glycol dimethacrylate.

eicosaethylene glycol hexadecyl ether), and Tween60 (poly(oxyethylene)-(20)-sorbitan monooleate), since they combine good accessibility and known phase behavior with weak interactions toward the resulting polymer gels. Furthermore, small quantities of such surfactants are known not to denature biological samples and can therefore be allowed to partially remain in the final gel.

In addition to the type of monomer and surfactant, both their concentrations during the polymerization as well as the cross-linking density of the resulting polymer networks were varied systematically, and the influence of all these parameters on the gel architecture were studied. The gel structures are characterized by scanning electron microscopy.

II. Experimental Section

II.1. Polymerization Procedure. Brij56, Brij58, and Tween60 were obtained from Fluka Co. and used as received; acrylamide, bis(acrylamide), *N*-isopropylacrylamide, glycidyl methacrylate, acrylic acid, and 2-hydroxyethyl methacrylate were supplied by Aldrich Co. The crystalline monomers were used as received; liquid monomers were purified by column filtration over Al_2O_3 in order to remove stabilizer and polymeric impurities.

The procedure of polymerization in lyotropic phases follows the classical recipes of radical polymerization. For instance, 0.75 g of Brij56 was mixed with 1.5 g of deionized water, to which a mixture of 0.75 g of acrylamide and 0.05 g of bis(acrylamide) (cross-linker) as well as 25 mg of potassium peroxodisulfate was added. Homogenization was carried out by shaking for 12 h. The mixture was polymerized by keeping the system at 55 °C for 12 h. The cross-linking density was varied between weight ratios of 1:3 and 1:100.

II.2. Characterization of the Reaction Mixture and the Gels. The phase behavior of the systems was examined by visual observation and polarized light optical microscopy before and during polymerization. To map the phase diagram, samples with different amounts of water and surfactant were prepared. The birefringence of lyotropic mesophases and their textures, used to identify hexagonal and lamellar structures, were observed by placing the samples between crossed polarizers of an Orthoplan-Pol microscope (Leitz) equipped with a hotstage.

Small-amplitude oscillatory shear measurements were conducted during polymerization using a Bohlin CVO-50 rheometer with cone-plate geometry (CP 1/40). A plate radius of 20 mm and a cone angle of 1° were used. The dynamic storage and loss moduli, G' and G'', were recorded at a polymerization temperature of 60 °C, in a shear frequency range between $0.005 < \omega < 100$ Hz and a strain of 0.02.

The morphologies of the final polymer gels, following purification and preparation by the critical-point drying method, were examined using scanning electron microscopy (SEM, Zeiss DSM 940). Samples were prepared as reported previously,[17,18] and it was already shown that this technique allows an artifact-poor visualization of the gel architecture in a dried state. The porous polymers were dried by the critical-point technique after a gradual exchange of the water for ethanol and finally for acetone.[19] The acetone was subsequently replaced by supercritical CO_2 using a BAL-TEC CPC 030. Throughout the procedure, the overall volume shrinkage of the gels is very low (below 10% at maximum), indicating the appropriate transformation of the solvent filled channel system to voids.

The dried and freeze-fractured samples were sputter-coated using a Pd/Ir target.

III. Results and Discussion

White or slightly opaque gels with good mechanical performance, which are easily handled in the solid state, were obtained in all experiments. Table 1 summarizes the compositions of the reaction mixtures of the samples described in this paper.

It should be noted that before polymerization all mixtures are transparent, and become opaque or turbid–white shortly into the reaction. Polarized-light optical microscopy reveals that most surfactant solutions (except for those where the surfactant concentration was

varied over a broader range) possess lyotropic order prior to addition of the monomer. The addition of monomer usually blurs the optical textures, indicating a decrease of order. The textures are, however, reestablished during polymerization. Systems with lower surfactant concentration start the polymerization reaction as a solution of globular micelles (L_1) but end up as strongly birefringent phases, corresponding to an increase of the surfactant concentration in a surfactant-rich phase during polymerization.

Small-angle X-ray scattering (SAXS) experiments on selected samples indicate that the surfactants preserve their order throughout the polymerization, although the peaks shift to higher scattering vectors and the related lower Bragg spacings.[20]

All these facts, as well as the strong increase in turbidity, suggest that the surfactant remains in a lyotropically ordered state, but expels the polymer from this phase. Both the coexisting polymer and surfactant-rich phases compete for the water, which leads (or does not lead) to a change of the lyotropic phase structure according to the binary phase diagram. The polymer gel is generated by cross-linking the phase, which is low in surfactant; therefore, the gel architecture is a result of demixing and not of the lyotropically ordered assemblies themselves acting as a template.

Scanning electron microscopy has been shown previously[17,18] to be the method of choice to search for the presence of large-scale demixing structures and to characterize gel structures on the micrometer scale. The series of micrographs in Figure 1 depicts the effects of monomer and surfactant variation on the gel structure in the final, purified state (complete conversion, surfactant removed). For these experiments, the abovementioned standard recipe was chosen, keeping other relevant parameters, such as concentrations and cross-linking density, constant so that just the chemical natures of monomer and surfactant were varied. In addition, we also show preparations of two standard gels which were made under similar conditions, but without any surfactant present. In the absence of surfactant, gels with glasslike fracture surfaces but without pronounced mesostructure are observed, proving the absence of major artifacts by the gel preparation technique, as well as the fact that the porosity is really due to the presence of the nonionic surfactant assemblies.

For all five monomers or monomer combinations, the choice of surfactant has only a marginal influence on the final gel structure. This result is somewhat unexpected, since the hydrophilicity and the spontaneous curvature changes from Brij56 (HLB 12.9) to Tween60 (HLB 14.9) and Brij58 (HLB 15.7). A wider variation of surfactants was not performed, since it was intended to start with a lamellar or hexagonal mesophase at initial polymerization conditions.

This independence confirms earlier observations[14−17] that for the nonionic surfactant systems the gel structure only indirectly depends on the morphology and structural properties of the lyotropic phase from which the reaction has started.

Variation of the monomer, however, has a strong influence on the structure of the resulting gels. For poly(acrylamide) (PAM), poly(*N*,*N*-dimethylacrylamide) (PDMAM) and poly(*N*-isopropylamide) (PNIPAM), it is observed that the whole structure consists primarily of small polymer spheres (ca. 500 nm in diameter). In the case of PAM and PDMAM, these spheres are cross-linked to form a rather continuous, mesoporous network. For PNIPAM, the primary spheres aggregate to clusters with graded branching but low overall connectivity ("cauliflower" morphology). Both structures obviously possess a quite large inner surface: BET measurements on the critical point dried samples resulted in specific surface areas of 7−20 m^2/g, depending on the sample. If we calculate from the specific surface area an "equivalant sphere size", this goes well with the particle size observed in SEM. This agreement also proves that the spheres are not porous by themselves (beside of the natural microporosity of all polymers, the so-called "solvent-pores"). It should also be noted that the "cauliflower-morphology" has already been observed for a number of other highly cross-linked acrylamide gels; see for instance ref 21.

In contrast, the copolymer poly(acrylic acid-*co*-glycidyl methacrylate) (PAA-*co*-PGMA) forms continuous gel structures of high connectivity, where the gel is composed of polymer strings. Both pore system and gel network are continuous. Poly(hydroxyethyl methacrylate) (PHEMA) adopts a gel morphology which is obviously constructed of porous sheets. It should be noted that a very similar morphology to the PHEMA gels has been observed for a product made from ternary microemulsions instead of lyotropic phases.[14,15] It should also be mentioned that the PNIPAM gels are the only ones in the series presented here which are mesostructured without even any surfactant present, since the polymer formed is water insoluble under polymerization conditions.

Explaining the different morphologies produced by varying the monomer is complex. Since the choice of monomer influences the interface energy between the demixing phases, the distribution of water between the two phases, the rheology of the two-phase system, as well as the polymerization kinetics and the time to reach gel transition, gel architecture is the product of a complicated balance. Although these results are perfectly reproducible, they do not allow a structural prediction of a new polymer gel derived from an analogue microphase-separated medium. We can only summarize that the gel structure is established kinetically and not according to more pretictable thermodynamic laws.

A remarkably interesting morphology for chromatographic applications is achieved from the combination of Tween 60 as the surfactant and the polymer PAA-*co*-PGMA. This morphology is best described by the series of higher-magnification SEM micrographs shown in Figure 2.

On a macroscopic level, the pore system consists of interconnected large spherical pores (ca. 10 μm in diameter), the cast of demixed and subsequently removed surfactant phase droplets. Additionally, the polymer-rich phase itself is porous and shows continuous channel systems on a length scale of ca. 200−400 nm. This second "tier" of pores is formed presumably during a second demixing step at a later stage of the reaction. It is known that carboxylates interact with nonionic surfactants, and therefore it can be speculated that these fine pores are caused by the complexed surfactants being expelled in a second step, which only occurs for Tween 60. The smallest building units of the gel observed using SEM are ca. 60 nm thick polymer rods scaffolding the gel. Since the copolymer is water-swellable, this network exhibits—unseen in SEM

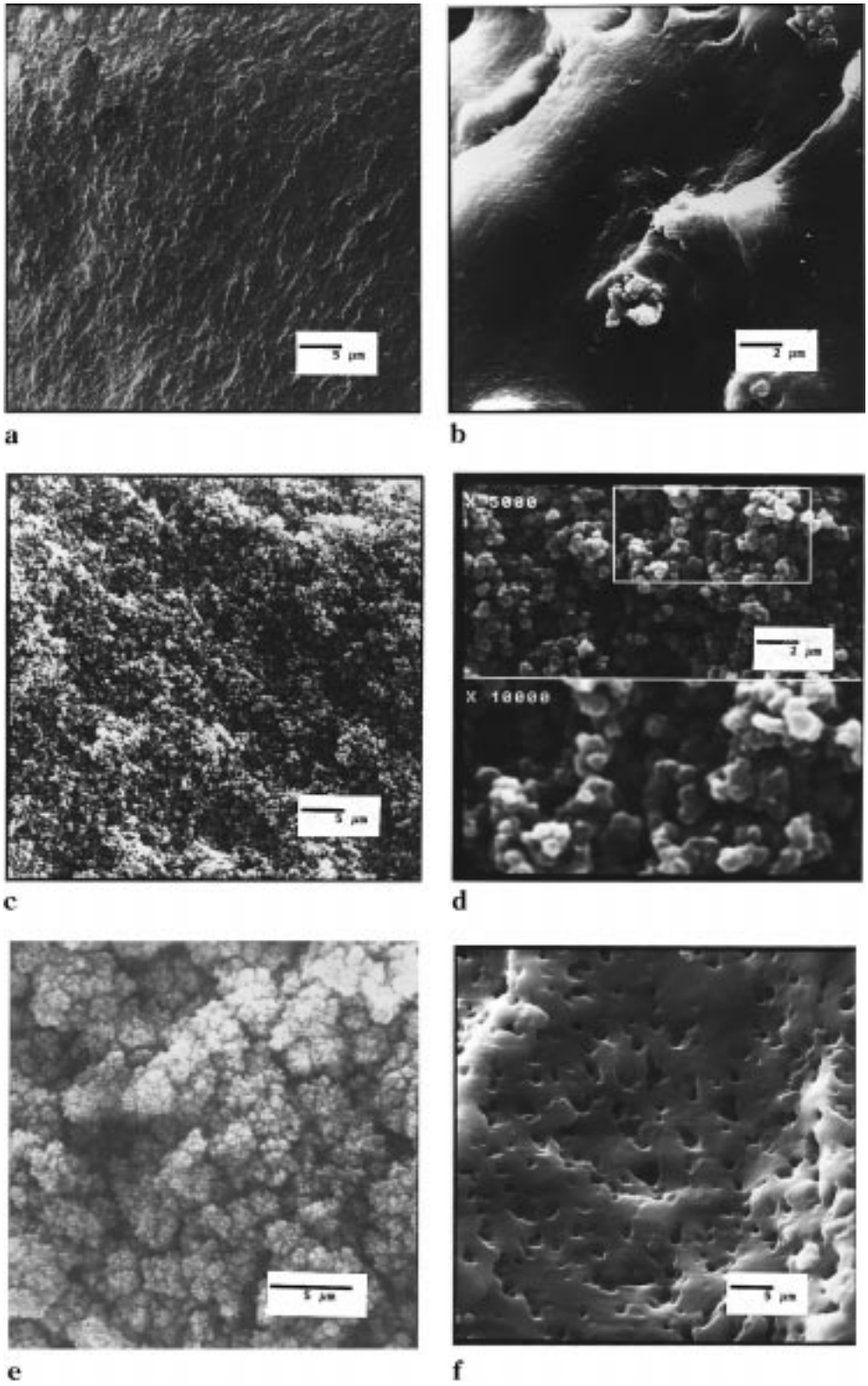

Figure 1. Scanning electron microscopy of critical point dried gel samples generated under various conditions: (a) acrylamide polymerized in the absence of surfactant, resulting in a wavy, but otherwise unstructured fracture surface; (b) poly(acrylic acid-*co*-glycidyl methacrylate) polymerized without surfactant results in glasslike fractures; (c) polyacrylamide gels made with Brij 56 (RAM-2) composed of small primary particles being continuously interconnected; (d) a similar structure, shown here in two higher magnifications, obtained for all poly(*N*,*N*-dimethylacrylamide) gels (here sample t3 made with Tween 60); (e) for poly(*N*-isopropylacrylamide), primary particles that are weakly and hierarchically interconnected, forming a "cauliflower" structure (GNP-9); (f) all PHEMA samples characterized by a morphology consisting of gel sheets or platelets with irregular pores (sample t2).

images—the usual molecular mesh size of a hydrogel. As a result, the structure possesses no less than three levels of pore structures. This architecture is very similar to the structure of some marine sponges, which rely on an optimized exchange of material with a liquid phase. Hierarchical pore structures have the advantage of both excellent flow transport and a high interface area for exchange due to the large and small pores, respec-

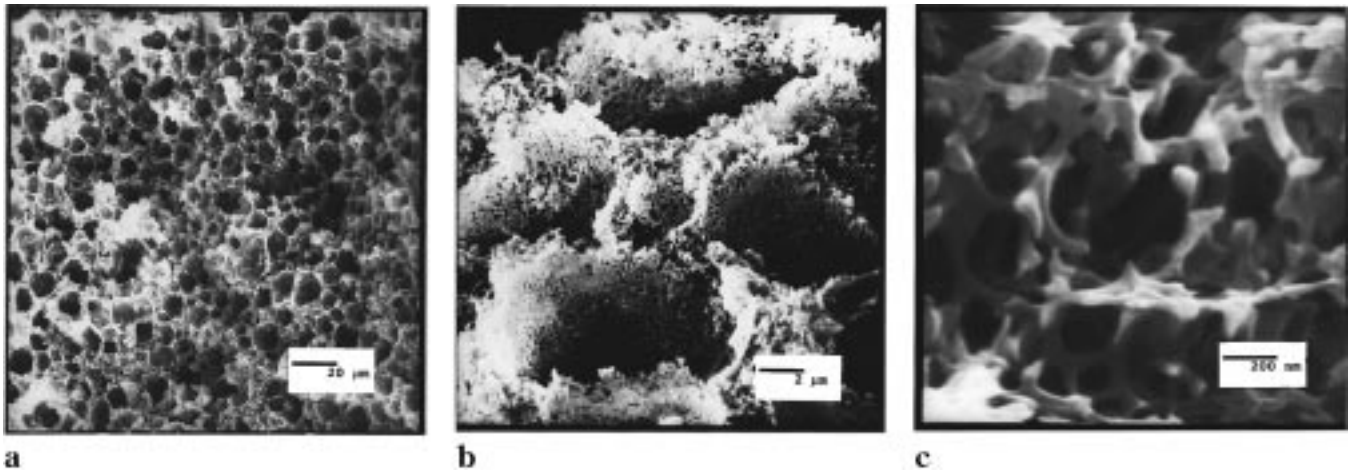

Figure 2. Zoom series of SEM pictures characterizing the hierarchical network setup of poly(acrylic acid)-*co*-polyglycidyl methacrylate, templated with Tween 60. It is seen that the gel consists of a dense packing of rather large spherical pores of ca. 10 μm (best seen in part a), separated by porous walls with channels 200 to 400 nm wide (part b). In the highest magnification it is seen that the primary mesoscopic element are gel strings with 60 nm diameter (part c).

Table 2. Storage Modulus *G′* and Loss Modulus *G″* of Some Gel Samples Characterizing Gel Strength and Connectivity[a]

		0.01 Hz		10 Hz	
sample	monomer	$G'/10^4$ pa	$G''/10^4$ pa	$G'/10^4$ pa	$G''/10^4$ pa
PAM-No	acrylamide	4.7	≪0.2	4.8	≪0.2
RAM-2		2.7	0.2	3.2	0.3
PDM-No	*N*,*N*-dimethyl-	4.5	≪0.2	4.5	≪0.2
RDA-2	acrylamide	3.1	0.2	4.1	0.1
PNIP-No	*N*-isopropyl-	1.1	≪0.2	1.3	≪0.2
RNP-2	acrylamide	0.08		0.21	0.18
PHE-No	hydroxyethyl	1.0	≪0.2	1.0	≪0.2
RHE-2	methacrylate	0.43	0.5	0.78	0.13

[a] Moduli are given for two different shear frequencies, and gels made without and with surfactant are directly compared.

tively. Since this gel structure is also highly functionalized (carboxylic acids and hydroxy groups from the opened epoxy rings), its structure is most attractive for adsorptive monolith chromatography.

The connectivity of the polymer backbone is also reflected in the frequency dependence of the elastic modulus. It is possible to charactize the structure of the swollen gel by its mechanical spectrum, since the response of smaller entities are observed at higher frequencies, whereas larger structures dominate at lower frequencies. The absolute modulus is proportional to the number of strands being involved in the mechanical strain, and therefore one can also determine the gel connectivity. Instead of presenting the whole set of moduli curves, Table 2 summarizes the storage (G') and loss part (G'') of the complex shear moduli of some selected networks at a low and a high frequency. In addition, these data are also compared with the reference samples being synthesized without surfactant, but under otherwise similar conditions.

All reference gels exhibit a comparably high modulus and low mechanical loss, as would be expected for gels without structural defects, being homogeneously water swollen. The absolute values of the storage modulus of $(1.0-4.7) \times 10^4$ pa change with the backbone density, i.e., the bulkier the side group, the lower the absolute modulus, and are typical for water-swollen, homogeneous gels with a polymer volume fraction of 0.25. Also from the rheological data, we can conclude that the reference gels are apparently not mesostructured.

The rheological behavior of the gels synthesized in the presence of surfactant show a completely different behavior which depends on the type of mesostructure. PMA and PDMAM networks show a reduction of the moduli by only 10−40%, as compared to the reference gels. At the same time they exhibit only a weak frequency dependence and low mechanical loss. The combination of these properties prove the regular and continuous nature of the gel mesostructure. The moduli of the PNIPAM gels strongly depend on the frequency plus the gels have a low absolute strength (about 1 order of magnitude lower than the reference sample), which is in good agreement with the shown "cauliflower" morphology and its related hierarchical branching.

At a first glance unexpected, the PHEMA gels have a low absolute modulus and a very high mechanical loss. Together with SEM, this suggests that the singular gel platelets are just weakly interlinked (allowing viscous dissipation), and that most of the cross-linker is consumed in the build-up of the gel sheets.

The influence of monomer concentration and cross-linking density on the network structure were studied for both the systems PAM/Brij 56 and glycidyl methacrylate/acrylic acid/Brij 58. Better imaging of the polymer gels is possible due to the more pronounced mesostructure of the copolymer system (Figure 3).

It is observed that the architecture or morphology of the system essentially does not depend on monomer concentration, whereas the size of the structure responds sensitively: the higher the monomer concentration, the smaller the pore diameters. BG-1 (17.8 wt % monomer) shows an average pore size of 2.5 μm, which decreases for BG-4 (24.4 wt % monomer) to 0.5 μm, and finally for BG-7 (29.9 wt %) to 0.3 μm.

Higher monomer concentrations increase the polymerization (and cross-linking) rate but slow the demixing dynamics by a higher viscosity, and the developing demixing structure for higher concentrations is obviously trapped in an earlier and more filigree state by the system crossing the gel point. Although this control of pore size is not a direct one, it can be used to reproducibly "tailor-make" the gel monolith's permeability and separation properties.

Unexpectedly, the influence of the amount of cross-linker present in the mixture is small: Both network topology and pore size remain essentially unaffected.

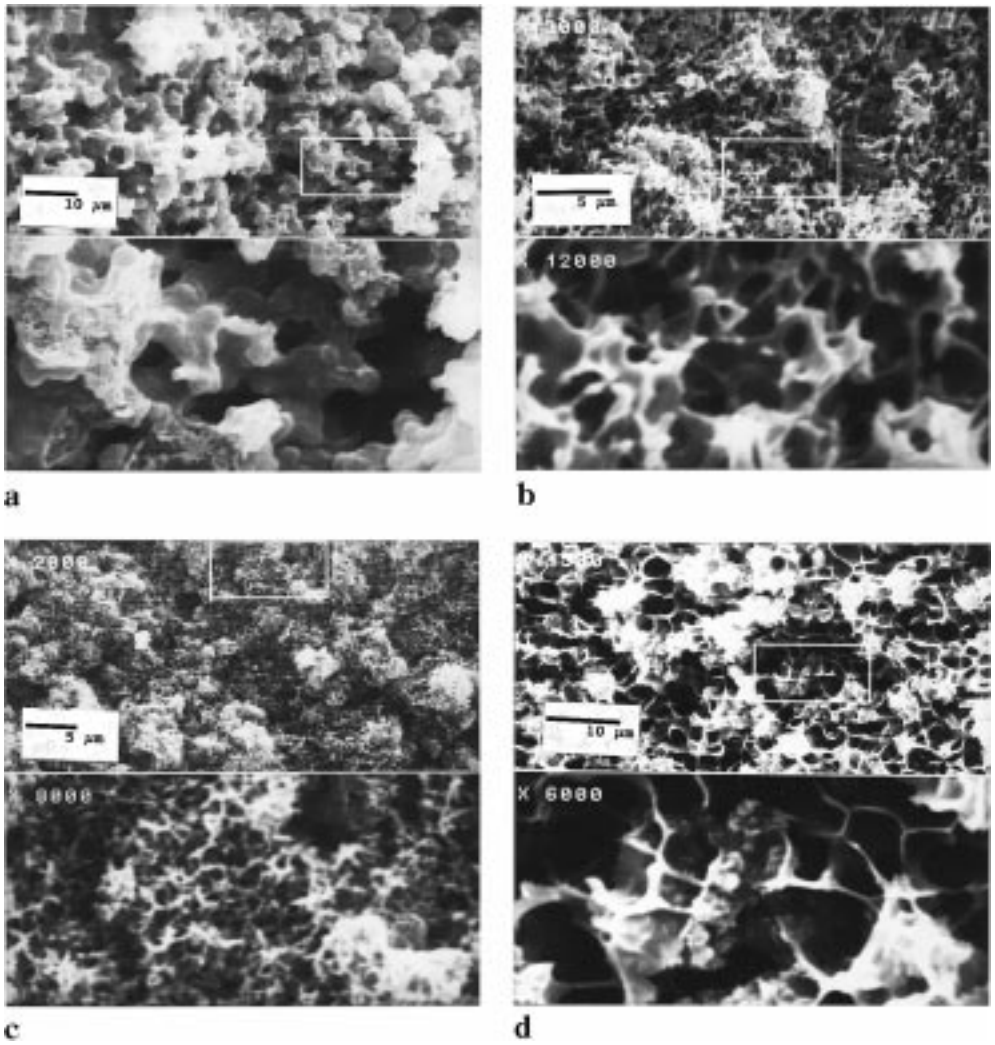

Figure 3. Scanning electron micrographs, characterizing the influence of monomer concentration and degree of cross-linking on the gel-structure of the system poly (acrylic acid-*co*-glycidyl methacrylate)/Brij 58: (a) A monomer content of 17.8 wt % results in a foamlike structure with a pore diameter of 2.5 μm (BG-1); (b) Increasing the concentration to 24.4 wt % results in a similar morphology with smaller pores of 0.5 μm (BG-4); (c) DA further increase of monomer concentration to 29.9 wt % (BG-7) finally results in pores of 300 nm size; (d) increasing the cross-linking density from 1/10 to 1/3 (BG-4 as compared to BG-6) only weakly changes pore size and architecture, but makes the gel-rods "more defined".

Only the gel strands look more defined, i.e., the interfaces are sharper, and the structure is more uniform with an increased amount of cross-linker. We attribute this structural refinement to the lower molecular swellability of highly cross-linked gels, which makes the growing gel strands richer in polymer. For gels with a low degree of cross-linking, we cannot be sure if the critical-point drying technique really depicts the gel as it is in the presence of water, since the molecular swellability might be sufficiently extensive to close a part of the mesoscopic pores.

Usually, increasing the amount of cross-linker also increases the rate of cross-linking, and a trend toward smaller pore sizes is expected. The fact that this dependence is not observed underlines that in the case of mesostructures, a differentiation between a local, molecular gel-point (within the droplets or strands) and a mesoscopic gel transition, describing the linking of the mesoscopic building blocks, needs to be made. While the first is dependent on the cross-linking ratio, the amount of cross-linker in the gel barely affects the latter.

Finally, it should again be mentioned that although the surfactant, monomer, and reaction conditions were varied over a wide range within the experiments presented here, in no case did the network structure follow the order and symmetry of the parental lyotropic surfactant phase. In most of the presented cases, the gelled reaction mixture obtained after polymerization did show the optical textures of a lyotropic phase, the structure of which could be confirmed by X-ray diffraction. All these indications of a locally ordered system, however, arise from the continuous surfactant subphase which acts as a porogen being embedded in a microscopically organized gel. This underlines the earlier observations of Chieng et al.[13,14] and Burban and Cussler.[18] There are reports claiming a successful mesostructuration, e.g., the work of Andersen and Strom[22] and that of Laversanne,[23] but in neither case were the purified and isolated gel structures characterized. Direct casting of a lyotropic phase by polymerization of nonstructure forming monomers is to our understanding still a task for future work with improved recipes and strategies.

IV. Conclusion and Outlook

It has been shown that polymerization reactions in the continuous water phase of lyotropic mesophases of nonionic surfactants allow the controlled generation of

highly ordered polymer gels. The gel structure, is not a cast of the original mesophase architecture, but exhibits structure elements 2 or 3 orders of magnitude larger than those addressed by the lyotropic assembly structure. This underlines previous observations that the structure formation is not directly caused by the surfactant aggregates but occurs due to demixing into a surfactant-rich and a polymer-rich subphases.

Variation of monomer and the type of surfactant revealed that the gel structure responds to the chemical structure of the formed polymer, but only weakly depends on the choice of surfactant. For PNIPAM, a "cauliflower" morphology was obtained, whereas PMA and PDMAM give continuous gel structures of high mechanical strength and connectivity being composed of spherical gel particles of ca. 500 nm diameter. PHEMA adopts a gel morphology consisting of porous sheets.

The size of these structures can be—within a certain range—adjusted by the monomer concentration: the higher the concentration, the smaller the pores. This is explained by crossing the gel transition in an earlier stage of the demixing, thereby fixing the structure. Increasing the amount of cross-linker mainly improves the sharpness of the structures, being better contoured at higher cross-linking densities

A very interesting gel morphology is found for PAA-*co*-PGMA, where a polymer gel with a hierarchical structure of three different kinds of pores and channels is found, resembling the morphology of a marine sponge. Such gels combine a very high surface area with excellent accessibility of all pores, an ideal prerequisite for the use in monolith chromatography. In addition, the described gel synthesis is a simple one-step procedure carried out within a short time which can be easily scaled up. It is therefore expected that such gels will be useful for a number of applications.

Acknowledgment. Project assistance with the closed pore systems was donated by ChezBriel PLC. Financial support from the Fonds der Chemischen Industrie and the Max-Planck-Society is gratefully acknowledged.

References and Notes

(1) *Pulsed field electrophoresis: A practical approach*; Monaco, A. P., Ed.; IRL Press: Cary, NC, 1995. *Electrophoresis in Practice: A Guide to Methods and Applications of DNA and Protein Separation*; Westermeier, R., Ed.; Wiley-VCH: New York, 1997.
(2) Abrams, I. M.; Miller, J. R. *React. Funct. Polym.* **1997**, *35*, 7.
(3) Peters, E. C.; Svec, F.; Frechet, J. M. J. *Chem. Mater.* **1997**, *9*, 1898.
(4) Stoffer, J. O.; Bone, T. *J. Polym. Sci. Polym. Chem. Ed.* **1980**, *18*, 264.
(5) Stoffer, J. O.; Bone, T. *J. Disp. Sci. Technol.* **1980**, *1*, 37; **1980**, *4*, 393.
(6) Vaskova, V.; Juranicova, V.; Barton, J. *Macromol. Chem. Macromol. Symp.* **1990**, *131*, 201.
(7) Gan, L. M.; Chew, C. H.; Friberg, S. E. *J. Macromol. Sci. Chem.* **1983**, *A19*, 739.
(8) Gan, L. M.; Chew, C. H.; Friberg, S. E.; Higashimura, T. *J. Polym. Sci., Polym. Chem. Ed.* **1981**, *19*, 1585.
(9) Gan, L. M.; Chew, C. H.; Friberg, S. E. *J. Polym. Sci., Polym. Chem. Ed.* **1983**, *21*, 513.
(10) Candau, F. In *Polymerization in Organized Media*; Paleos, C. M., Ed.; Gordon Science Publ.: Philadelphia, PA, 1992; p 215.
(11) Antonietti, M.; Basten, R.; Lohmann; S. *Macromol. Chem. Phys.* **1995**, *196*, 441.
(12) Palani Raj, W. R.; Sasthav, M.; Cheung, H. M. *Polymer* **1993**, *34*, 3305 and references cited therein.
(13) Chieng, T. H.; Gan, L. M.; Chew, C. H.; Lee, L.; Ng, S. C.; Pey, K. L.; Grant, D. *Langmuir* **1995**, *11*, 3321.
(14) Chieng, T. H.; Gan, L. M.; Chew, C. H.; Ng, S. C.; Pey, K. L. *J. Appl. Polym. Sci.* **1996**, *60*, 1561.
(15) Chieng, T. H.; Gan, L. M.; Chew, C. H.; Ng, S. C. *Polymer* **1995**, *36*, 1941.
(16) Antonietti, M.; Hentze, H. P. *Colloid Polym. Sci.* **1996**, *274*, 696.
(17) Antonietti, M.; Hentze, H. P. *Langmuir* **1998**, *14*, 2670.
(18) Burban, J. H.; He, M.; Cussler, E. L. *AIChE J.* **1995**, *41*, 907.
(19) Reimer, L.; Pfefferkorn, G. *Scanning Electron Microscopy*; Springer: Berlin, 1972.
(20) Weissenberger, M. Doctoral Thesis, Potsdam, 1998.
(21) Xie, S. F.; Svec, F.; Frechet, J. M. J. *J. Polym. Sci., Polym. Chem. Ed.* **1997**, *35*, 1013.
(22) Strom, P.; Anderson, D. M. *Langmuir* **1992**, *8*, 961.
(23) Laversanne, R. *Macromolecules* **1992**, *25*, 489.

MA9812478